

Mathematical modeling of Ka-226 / Ka-26 helicopter main rotor blade flapping motion at rotor acceleration / deceleration in wind conditions



Boris N. Burtsev
*Aeroelastic Blade Design
Department Chief*



Vladimir I. Ryabov
*Aeroelasticity Group
Loading Engineer*



Sergey V. Selemenev
*Aeroelasticity & Rotor Design
Department Director*

Kamov Company, Russia

Results of evaluating the effect of wind speed and direction upon the Ka-226/Ka-26 helicopter main rotor blade flapping motion are presented. These results are obtained by modeling of rotor acceleration/deceleration conditions at the engine start up and shut down at constant wind speed. Rotor speed versus time values are taken from real rotor acceleration/deceleration test data. The ULYSS-6 mathematical model of a coaxial rotor with elastic blades and elastic control linkage with time variable limit conditions in the root section (leaving the droop stop and return to the droop stop) is used. A system of flexible blade equations is integrated together with a coaxial rotor nonlinear vortex model. The results obtained are compared with experimental data.

Notation

X_K, X_B	pilot's cyclic stick positions, deg.
X_H, φ_{OH}	pedal position, collective pitch, deg.
n_R	rotor speed, %
Y_U, Y_L	blade tip coordinates relative to the lower rotor hub rotation plane, mm
H	upper blade tip to lower blade tip clearance, mm
W	wind speed, m/sec
α, β	angle of attack, slip angle, deg.
ψ	lower rotor blades azimuth angle, deg.

Abbreviation and Subscripts

U, L	upper, lower
UR, LR	upper rotor, lower rotor
HRP	rotor hub rotation plane
RFM	Rotorcraft Flight Manual

Coordinates systems and signs convention are presented in Fig.1.

Distance ($H = Y_U - Y_L$) between upper/lower rotor blade tips is determined at six (6) azimuth "meeting" (ψ_1, \dots, ψ_6) points of the upper/lower rotor blades (ref. to Fig.2).

Introduction

One of the main tasks in determining safe boundaries of helicopter operating under wind conditions is analysis of flapping motion and clearance between coaxial rotor blade tips at acceleration up to operating speed before take-off and deceleration of the rotor after landing.

At acceleration/deceleration the opportunity for significant flapping motion of the blades in the vertical plane appears because of the little centrifugal unloading and as a result - decrease of clearance between tips of the upper and lower coaxial rotor blades and decrease of clearance between rotor blades and helicopter fuselage structural elements as well.

Acceleration/deceleration of the rotor is being limited, mainly, by wind conditions on the runway. Included into the Flight Manual maximum airflow speed limitation (W_{max}) at acceleration/deceleration of the rotor is defined by the structure and elastic/mass configuration of the rotor system of every type of the helicopter.

Kamov Company's specialists from the aeroelasticity team develop calculation methods and numerical simulation of the rotor acceleration/deceleration under wind conditions from 1988. The largest volume of calculations was carried out in the years of 2003...2007 for the Ka-26 and Ka-226 helicopters.

The main results of research work for the Ka-26 and Ka-226 coaxial helicopters are presented in this paper (ref. Table 1).

The Ka-26 helicopter developed by specialists of the design bureau under the leadership of N.I. Kamov lifted off in May 1965 and in August, 18-th it performed its first circular flight. The outstanding designer M.A. Kupfer was at the beginnings of the Ka-26 helicopter development. The helicopter was successful and its fiber glass reinforced plastic rotor blades became really revolutionary solution that determined in advance for not less than 15÷20 years [7] tendency of world development of composite materials and technology of composite blades manufacturing. Aircraft industry manufactured more than eight hundred Ka-26 helicopters. At present around thirty hundred Ka-26 helicopters are under operation in Russia and abroad.

Multifunctional Ka-226 helicopter is a successor of the Ka-26 helicopter now. Prototype of the Ka-226 helicopter (with rotor system

from Ka-26) performed its maiden flight in September 4, 1997. Specialists of the design bureau created a new rotor system for the Ka-226 helicopter. In the structure of the rotor hubs data from the Ka-50 and Ka-62 perspective programs are used. Fiber glass carbon plastics blades of new generation are developed for the Ka-226 helicopter with improved aerodynamic and elastic/mass configuration [7]. The first flight with the new rotor system was performed in March 28, 2001. New rotor system and powerplant provided significant growth of the Ka-226 helicopter performance in comparison with the Ka-26 helicopter. Delivery of the first mass-produced Ka-226 helicopters to operators began in 2004.

ULYSS-6 mathematical model

The ULYSS-6 general mathematical model for calculating loads and rigidity of coaxial rotor system motion was created at Kamov Company with the purpose to solve general problems of aeroelasticity [1÷7].

The present model combines: mathematical model of coaxial rotors with elastic blades, model of elastic control linkage, coaxial rotor vortex model. The mathematical model is shown in Table 2.

Model-based aeroelastic phenomena are presented by means of line 1 and columns 2÷5 in Table 2, and namely:

- line 1 – conventionally reflects non-linearity, periodicity and “parametrizm” of coefficients in the system of equations of rotor blades motion;
- column 2 – part of the boundary conditions of the system of equations, modeling elastic connection - consistency of blade roots turns in the control linkage under blade twisting effects;
- column 3 – aeroelastic interference of coaxial rotor blades through coaxial rotor vortex modeling (i.e. for calculating air force – attack angles in blade sections);
- column 4 – force and moment coefficients on airfoils in blade sections subject to attack angle and Mach number and their time derivatives according to data obtained at tests of airfoils in stationary and non-stationary flow in aerodynamic tunnels; possible registration of deformations in tail part of blade airfoil;

- column 5 – elastic/mass and geometric data of upper/lower rotor blades and hubs.

Functional capabilities of the model are shown in the lower line of Table 2, at the same time the following is calculated:

- summarized and distributed loads, blades bending and torsional moments;
- upper/lower rotor hubs variable and constant forces and moments;
- control system loads – rotors control linkage and operating rods of the actuators;
- geometrical parameters of the elastic blades motion – flapping motion of upper/lower rotor blades and \ between blades tips;
- stability limit of “stall flutter” type;
- stability limit of “transonic flutter” type in forward flight and during ground testing;
- Helicopter Performance.

The basis of the mathematical model is composed of the system of three non-linear differential equations of a single elastic rotor blade motion in partial derivatives with periodical coefficients relatively to blades motion and limit conditions of the control linkage joint elastic twisting. Equations of motion were obtained by B.N. Burtsev with the use of the least action principle in Hamilton form and were published earlier in the papers [1, 4, 7].

The ULYSS-6 mathematical model of the coaxial rotors for numerical simulation of acceleration/deceleration of the rotor under wind conditions was specially updated:

- Basic algorithm of the ULYSS-6 model was updated as to approximation of discontinuous functions of the blade linear characteristics;
- Modeling of the oblique flow around blade (sliding flow) is included;
- Variable limit conditions in the blade root are taken into account: fixed blade root, when blade is on the droop stop; and feathering hinge with friction, when blade does not touch droop stops;
- Modeling of gust is included;
- Graphic portion of calculation results is developed.

Main results

Adequacy of mathematical model

Fig.3, 4 show comparison of the Ka-26 helicopter rotors acceleration/deceleration mathematical modeling results in wind of $W=15$ m/sec with actual test results. It is seen that calculation results coordinate with test results both on the blade motion character and on the values of flapping motion of the upper/lower rotor blades at azimuth meeting points.

The Ka-26 helicopter acceleration / deceleration calculation results confirm correctness of the ULYSS-6 mathematical model work and demonstrate possibility to predict for certain behavior of new blades under wind condition prior to testing.

Resonance character of elastic blades flapping motion

By means of numerical simulation according to the ULYSS-6 mathematical model within the rotor speed of $n_R = 5...20\%$ resonance character of flapping motion of the Ka-26 and Ka-226 helicopters coaxial rotor elastic blades was revealed. Decrease of the minimum clearance between blade tips of the upper/lower rotors of the Ka-26 helicopter down to 500 mm and wind velocity of $W=20$ m/sec at the rotor speed of $n_R < 15\%$ is stipulated by the resonance character of blades flapping motion with this speed (ref. to Fig.5). Two frequency peaks in amplitudes of the 2-nd and 3-d harmonics of blade tips flapping motion were revealed (ref. to Fig.6, 8) by means of calculations for the Ka-26 and Ka-226 helicopters. By increase of rotor speed (rpm) from 5% up to 20% the blades, which lay on the droop stops, sequentially appear to be in resonance with the 3-d and 2-nd excitation force harmonics. These forces excite flap motion at frequency of ~ 1 Hz, that is the frequency of the first elastic tone of the blade at the droop stop.

Fig.7, 9 show frequency diagrams of the Ka-26 and Ka-226 helicopters rotor blades that were calculated with the use of another method – MFE aeroelastic mathematical model.

MFE mathematical model [5, 7] was developed at Kamov Company with the purpose to solve general problems of aeroelastic stability and jointly with the ULYSS-6 mathematical

model presents integrated mathematical model of the coaxial aeroelastic rotor. The MFE program permits to model motion of a single rotating elastic blade by means of method of final elements (MFE). At the same time frequencies, forms and stability of blade vibration in vacuum and in the air are calculated.

From Fig.7, 9 it is seen that as in the calculation according to the ULYSS-6 (ref. to Fig.6, 8) at the rotor speed of $n_R < 20\%$ the first tone of blade flapping vibration appears to be in resonance with the 3-d and 2-nd excitation force harmonics (blade roots are fixed at the droop stops).

Wind gust modeling

Effect of wind gusts on the Ka-226 helicopter upper/lower rotor blades flapping motion value was analyzed only for the cases with resonance values of rotor speed under head wind conditions. Single "cosine" wind gust is added to values of wind speed in the calculation of the steady flight at constant wind speed and constant rotor speed (ref. to Fig.10).

Fig.11 presents results of comparison of calculations with wind gusts and without wind gusts. Modeling of wind gust made for constant wind speed of $W_0=20$ m/sec. plus single "cosine" wind gust of $A_{gust}=5$ m/sec demonstrated that maximum effect of wind gust corresponds to the effect of constant wind speed increased by gust value (25 m/sec = 20 m/sec + 5 m/sec) and does not depend on gust duration (Tgust).

Parametric research

By means of numerical simulation of the Ka-226 helicopter rotors acceleration / deceleration under wind conditions dependence of minimum clearance between the coaxial rotor blade tips was received on:

- constant wind speed and at wind gusts;
- wind direction;
- angle of blade sleeve droop stops;
- angle of attack of rotor;
- controls position (φ_{OIII} , X_H , X_B , X_K).

Calculated limitation of the allowable wind speeds at rotors acceleration/deceleration in dependence to wind direction (ref. to Fig.12) was received.

Conclusions

1. Method of calculating coaxial rotor blades flapping motion at acceleration/deceleration under wind conditions was developed.

In the method of calculating it was used:

- time dependencies of rotor speed out of test results;
- mathematical model of coaxial rotors with elastic blades on the elastic control linkage with variable limit conditions in the blade root (leaving the droop stop and return to the droop stop);
- vortex model of the coaxial rotors;
- model of the blade airfoil airflow with dynamic pulling of stall and consideration of oblique airflow.

2. The method was tested by means of modeling of the Ka-26 helicopter rotor acceleration/deceleration at wind of $W=15$ m/sec with repetition of testing conditions. The results of modeling coordinate well with the results of the Ka-26 actual tests, so adequacy of the developed calculating method is confirmed.

3. Resonance character of the coaxial rotor elastic blades flapping motion of the Ka-26 and Ka-226 helicopters was revealed by means of the numerical simulation within the range of the rotor speeds of $n_R=5...20\%$. Decrease of the minimum clearance between the upper/lower rotor blade tips is due to the resonance character of the blades flapping motion at these speeds.

4. Effect of the horizontal wind gust on the Ka-226 helicopter rotor blades flapping motion at acceleration/deceleration was calculated. Modeling of wind gusts demonstrated, that maximum gust effect corresponds to constant wind speed effect increased by gust value ($W = W_0 + A_{gust}$) and does not depend on the gust duration (time).

5. The Ka-226 helicopter rotors acceleration/deceleration calculations were conducted. Blades flapping motion at different speeds and direction of wind was predicted. On the basis of the calculations recommendations on acceleration/deceleration of the Ka-226 helicopter rotors were formulated for pilots.

6. At present the developed method is used at Kamov Company for modeling rotors acceleration/deceleration under wind conditions with the purpose to optimize rotor systems design, to determine and extend operating limitations.

References

¹ Bourtsev B.N., “Aeroelasticity of Coaxial Helicopter Rotor”, *Proceedings of 17th European Rotorcraft Forum*, Germany, Berlin, Sept. 1991, p.p. 435÷451.

² Bourtsev B.N., “The Coaxial Helicopter Vibration Reduction”, *Proceedings of 18th European Rotorcraft Forum*, Avignon, France, Sept. 1992.

³ Bourtsev, B.N., Selemenev, S.V., “The Flap Motion and the Upper Rotor Blades to Lower Rotor Blades Clearance for the Coaxial Helicopters”, *Proceedings of 19th European Rotorcraft Forum*, Italy, Como, Sept. 1993.

⁴ Bourtsev, B.N., Selemenev, S.V., “The Flap Motion and the Upper Rotor Blades to Lower Rotor Blades Clearance for the Coaxial Helicopters”, *Journal of the AHS*, Vol.41-No.1, January 1996, p.p. 37÷51.

⁵ Bourtsev, B.N., Selemenev, S.V., Vagis, V.P., “Coaxial Helicopter Rotor Design & Aeromechanics”, *Proceedings of 25th European Rotorcraft Forum*, Vol.1, Italy, Rome, 14-16 Sept. 1999, p.p. G22-1÷20.

⁶ Bourtsev, B.N., Ryabov, V.I., Selemenev, S.V., Butov, V.P., “Helicopter Wake Form Visualization Results and their Application to Coaxial Rotor Analysis at Hover”, *Proceedings of 27th European Rotorcraft Forum*, Russia, Moscow, 11 - 14 Sept. 2001, p.p. 64.1÷13.

⁷ Mikheyev, S.V., Bourtsev, B.N., Danilkina, V.L., Ivannikova, R.V., Selemenev, S.V., Schetinina, Y.S., “Kamov Composite Blades”, *Proceedings of 31st European Rotorcraft Forum*, Italy, Florence, 13 - 15 Sept. 2005, p.p. No.3-1÷22.

Systems of Coordinates & Sign Convention

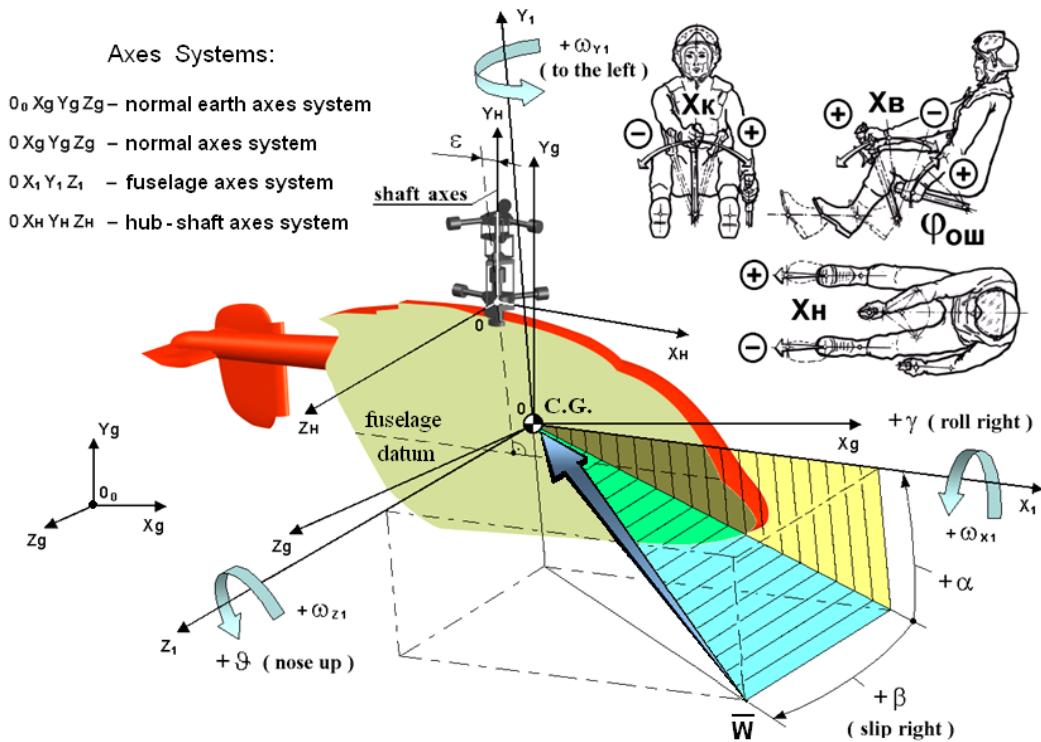


Fig.1

Upper / Lower rotor blade tip meeting point coordinates

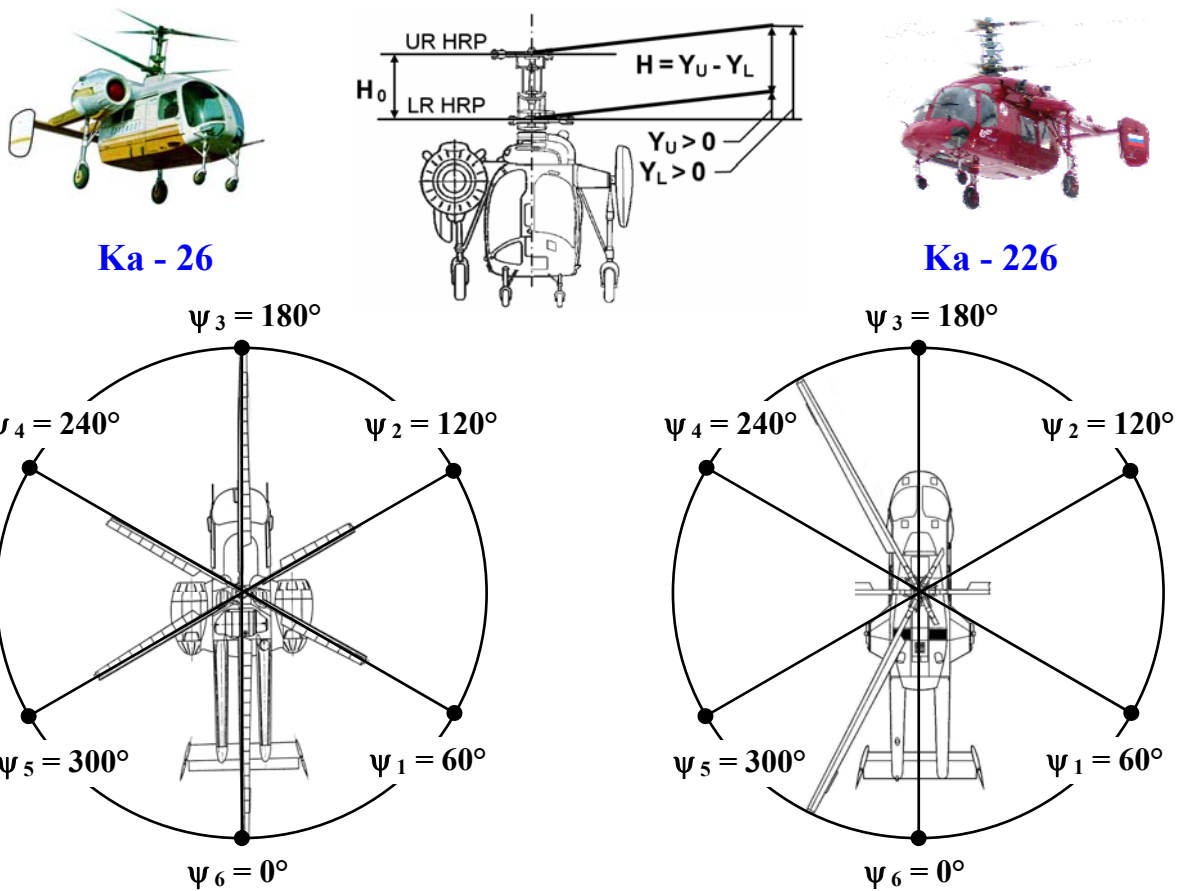


Fig.2

Basic Ka-26, Ka-226 Data & Main Rotor Data

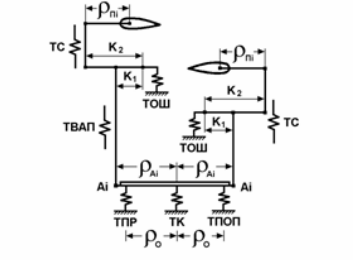
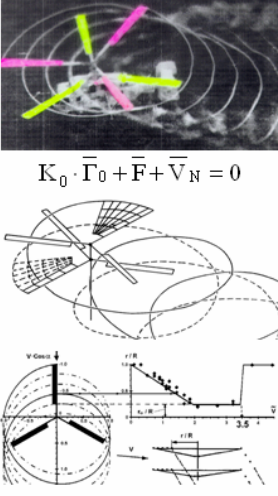
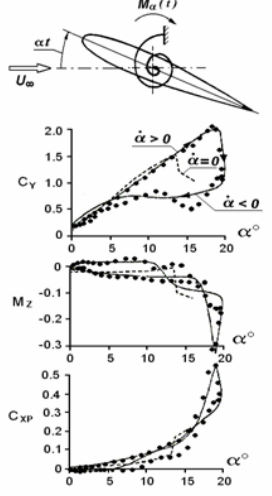
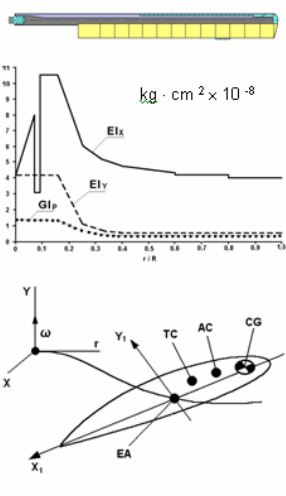
Table 1.

Parameter	Notation	Dimension	Ka - 26	Ka - 226
T-O weight	W_{T-O}	kg	3250	3400
Engine type (T-O power)	- P	- (h.p.)	M-14B26 (2 × 325)	Allison 250-C20R/2 (2 × 450)
Main rotor disk loading	$W_{T-O} / (\pi R^2)$	kg / m ²	24.5	25.6
Power loading	W_{T-O} / P	kg / h.p.	5	3.8
Rotor radius	R	m	6.5	6.5
Upper / Lower rotor hub distance	H_0 ($\bar{H}_0 = H_0 / R$)	m (-)	1.170 (0.180)	1.142 (0.176)
Number of blades	k_B	-	3 + 3	3 + 3
Rotor blade chord ($r / R = 0.7$)	c_7	m	0.25	0.26
Rotor solidity	$\sigma_7 = k_B \cdot c_7 / (\pi R)$	-	0.0735	0.0764
Blade twist	$\Delta \varphi_\Sigma$	deg	- 11.6 (non-linear)	- 8.17 (linear)
Blade taper	c_0 / c_K	-	2 : 1	1 : 1
Blade airfoil	-	-	NACA 230	TsAGI - 4M
Lock number *	γ_B	-	5.56	2.91
Rotor tip speed (rotor speed)	ωR (n_R)	m / sec (%)	178 (87)	192.6 (100)

*) Notes: $\gamma_B = c_7 \cdot \Delta \cdot a_\infty \cdot R^4 / (16 \cdot I_\beta (\text{kg} \cdot \text{m} \cdot \text{sec}^2))$ (ISA SLS, relative air density: $\Delta = 1$).

Modeled aeroelastic phenomena & Functional capabilities of ULYSS-6 code

Table 2.

Simulated Aeroelastic Phenomena of Coaxial Rotor			
1. System of equations of coaxial rotor blades motion : $EI_x (r / R , \omega t)$, $EI_y (r / R , \omega t)$, $GI_p (r / R , \omega t)$			
<p>2. Elastic model of coaxial rotor control linkage (boundary data)</p> <p style="text-align: center;">$\bar{\varphi} = \parallel \Phi_{T,L} \parallel \times \bar{M}$</p> <p style="text-align: center;">Variable control linkage rigidity</p>	<p>3. Model of coaxial rotor vortex wake</p> <p style="text-align: center;">$V_i (r / R , \psi)$</p> <p style="text-align: center;">Non-linear blade vortex theory</p>	<p>4. Steady and unsteady aerodynamic airfoils data</p> <p style="text-align: center;">$C_Y, M_Z, C_{XP} (\alpha, M, \dot{\alpha}, \ddot{M})$ $C_{Y_MAX} (\alpha, \dot{\alpha}, M)$</p>	<p>5. Elastic / mass / geometry data of the upper / lower rotor blades and of the hubs</p>
			
Functional capabilities			
Loads & Deformation, Blade flap motion & Blade tips clearances	Aeroelastic stability limits: stall flutter, transonic flutter, ground resonance	Helicopter performance & maneuverability	

Ka-26. Rotor acceleration. Comparison between analysis and test results

Upper / Lower rotor blade tip flap motions at meeting azimuth points

Head wind: $W = 15 \text{ m/sec}$, $\alpha = -6^\circ$, $\varphi_{OIII} = 0^\circ$, $X_B = 4.3^\circ$, $X_H = 0^\circ$

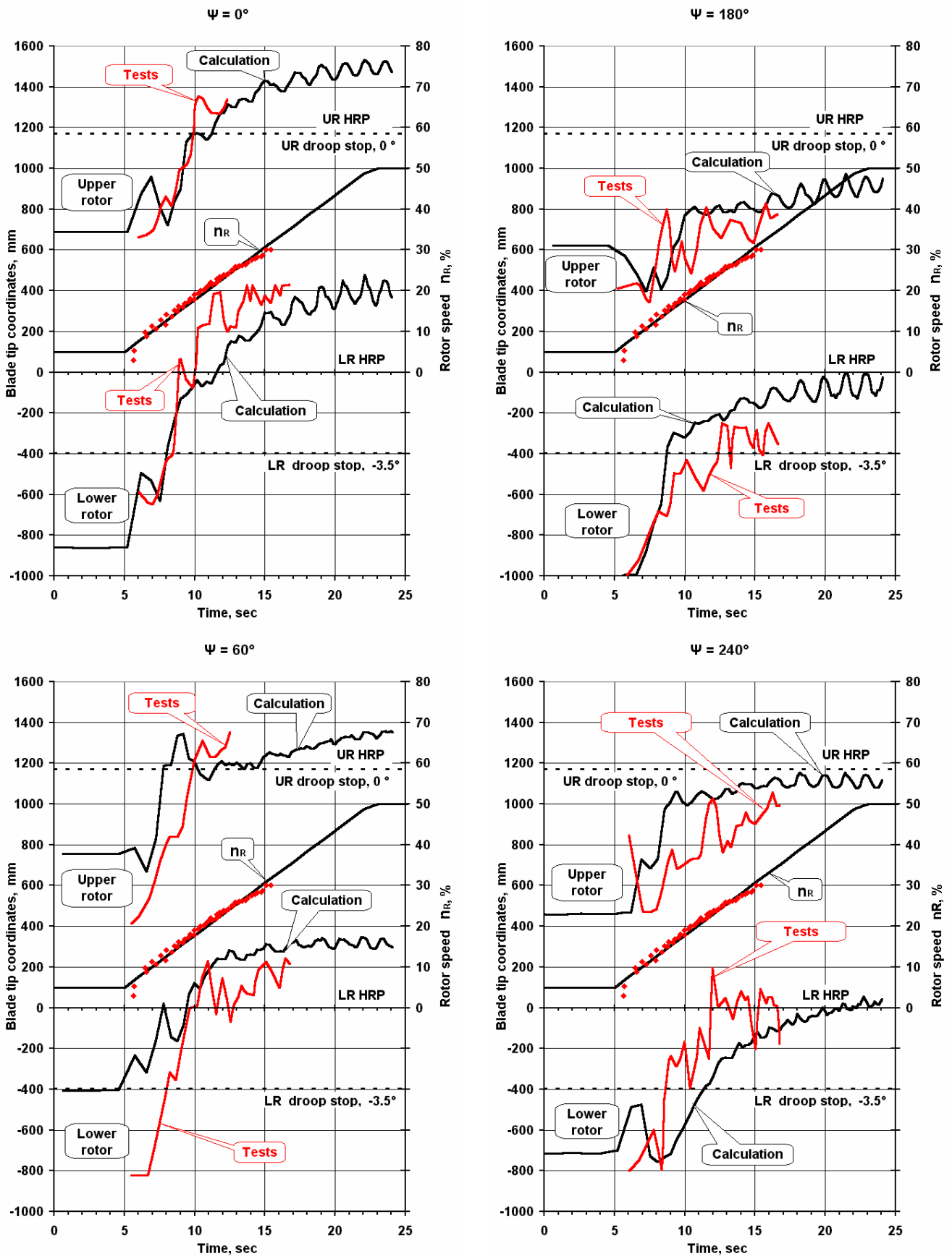


Fig.3

Ka-26. Rotor deceleration. Comparison between analysis and test results

Upper / Lower rotor blade tip flap motions at meeting azimuth points

Head wind: $W = 15 \text{ m/sec}$, $\alpha = -6^\circ$, $\varphi_{OIII} = 0^\circ$, $X_B = 4.3^\circ$, $X_H = 0^\circ$

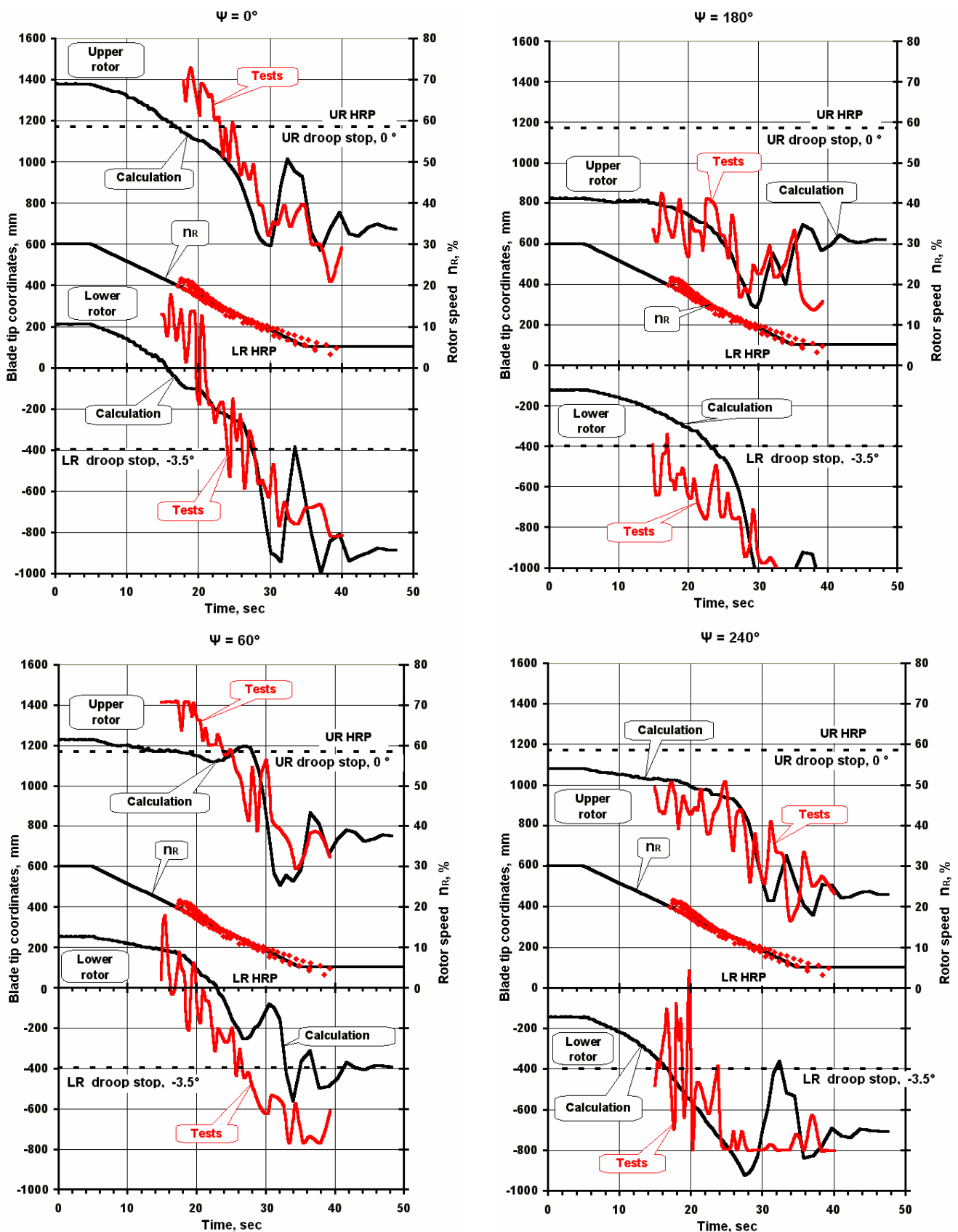


Fig.4

Ka-26. Calculations with constant rotor speed

Blade tip flap motion and blade tip clearance versus azimuth

Head wind: $W = 20 \text{ m/sec}$, $\alpha = -6^\circ$, $\varphi_{OH} = 0^\circ$, $X_B = 4.3^\circ$, $X_H = -1.5^\circ$

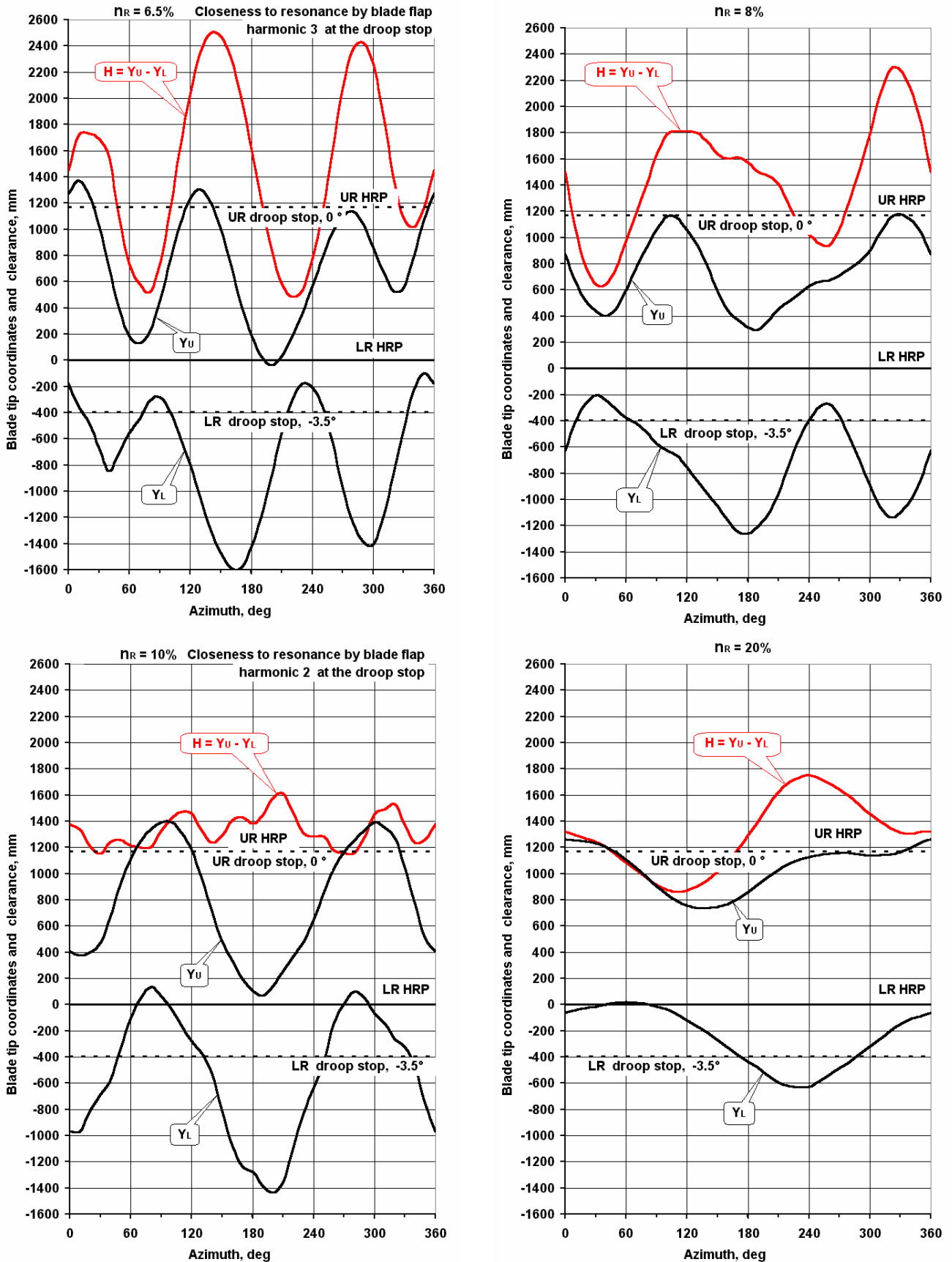


Fig.5

Ka-26. Calculations with constant rotor speed

Blade tip flap harmonic amplitudes

Head wind: $W = 20$ m/sec, $\alpha = -6^\circ$, $\varphi_{OIII} = 4.3^\circ$, $X_B = 0^\circ$, $X_H = -1.5^\circ$

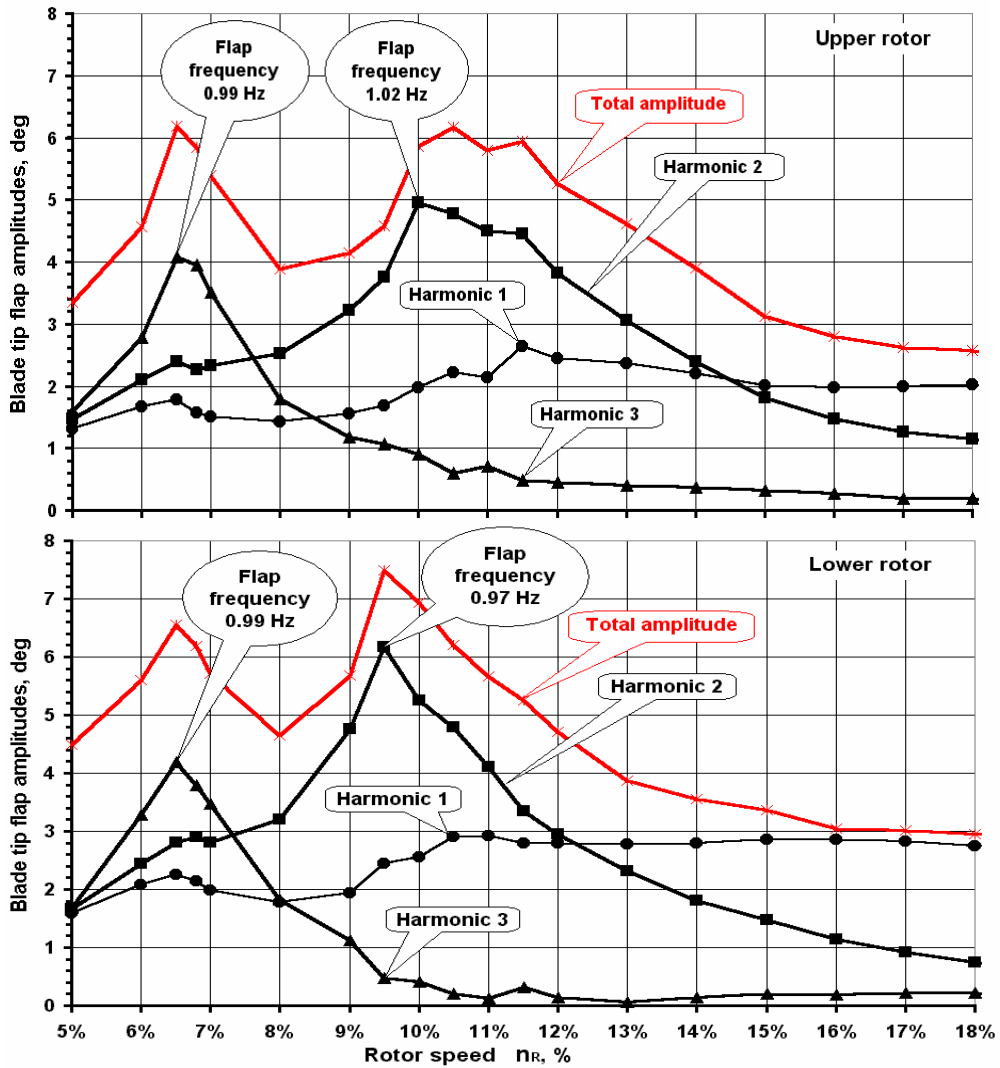


Fig.6

Ka-26. Frequency diagram

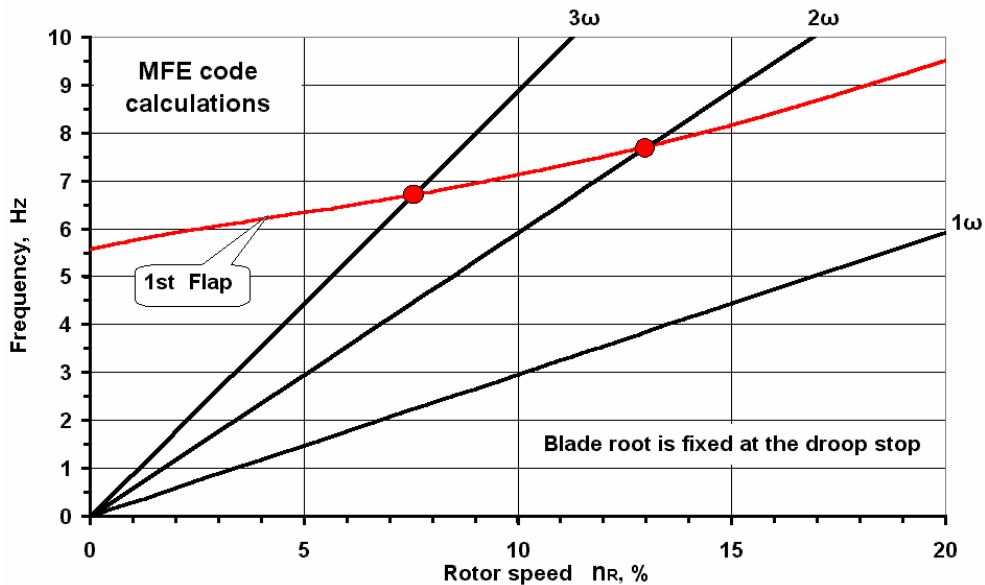


Fig.7

Ka-226. Calculations with constant rotor speed Blade tip flap harmonic amplitudes

Head wind: $W = 25 \text{ m/sec}$, $\alpha = -6^\circ$, $\varphi_{OIII} = 0^\circ$, $X_B = 0^\circ$, $X_H = 0^\circ$

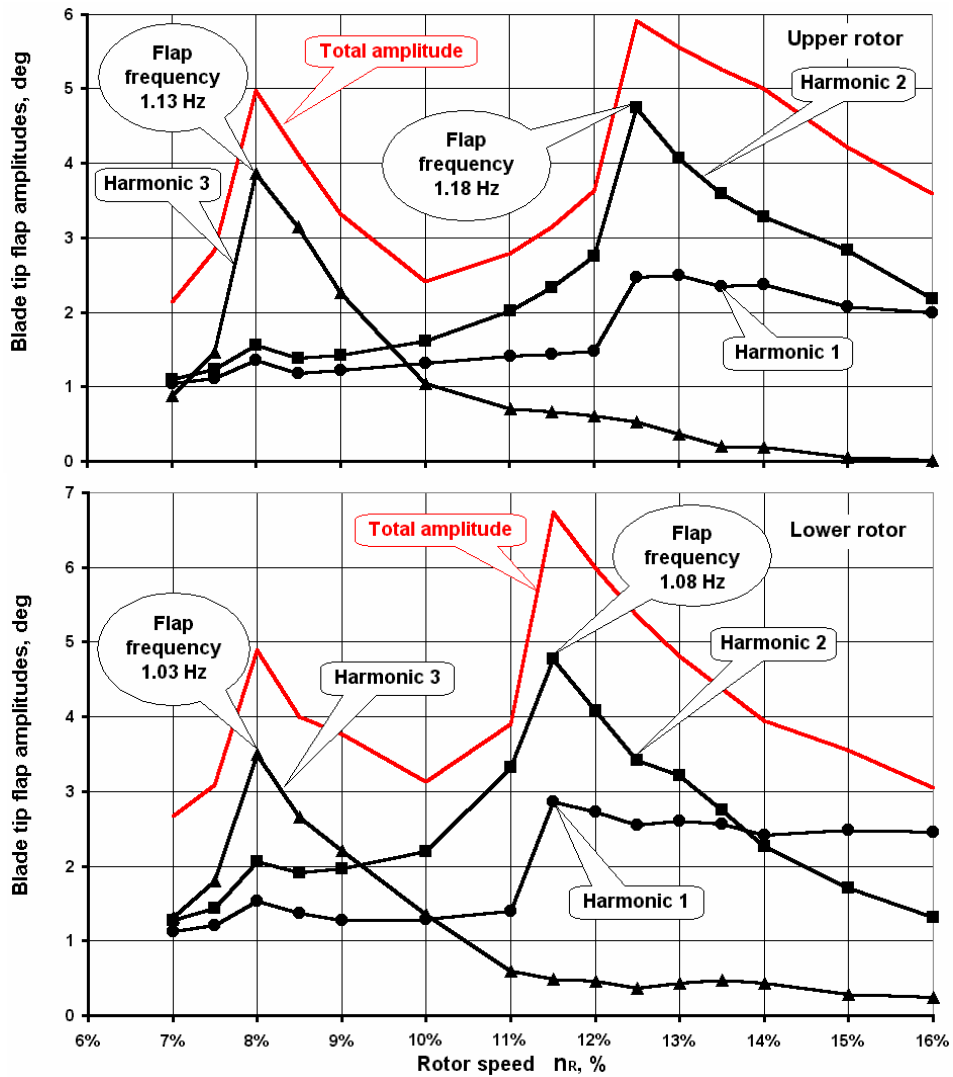


Fig.8

Ka-226. Frequency diagram

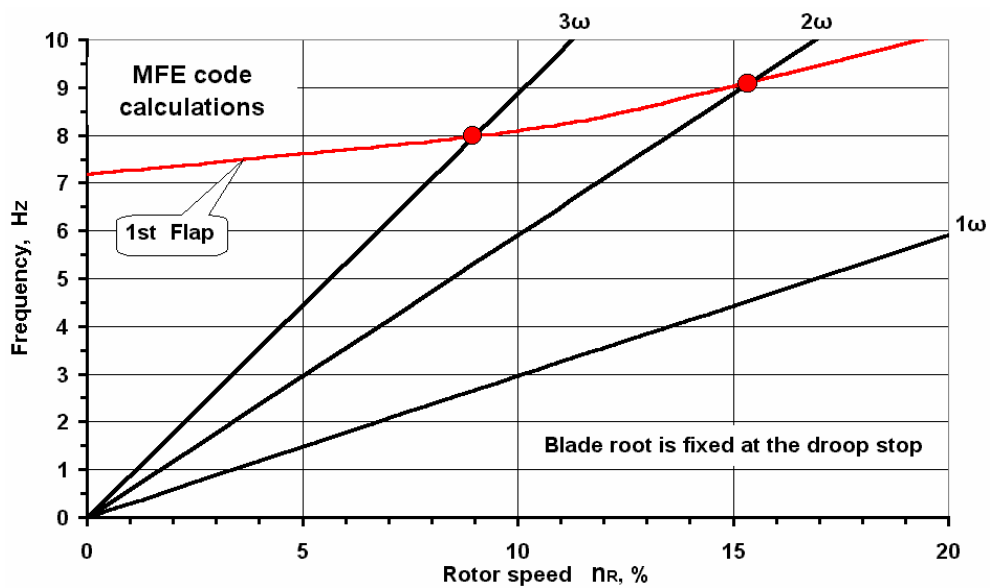


Fig.9

Wind gust profile

$$W(t) = W_0 + A_{gust} \cdot [1 - \text{Cos}(2\pi(t - t_1) / T_{gust})] / 2,$$

for: $t_1 \leq t \leq (t_1 + T_{gust})$;

$$W(t) = W_0,$$

for: $(t_1 + T_{gust}) < t < t_1$,

where:

$W_0 = 20$ m/sec - wind speed permanent component;

$A_{gust} = 5$ m/sec - ax value of speed increase in the gust;

t_1 - gust starting moment;

t - current time value;

T_{gust} - duration of gust.

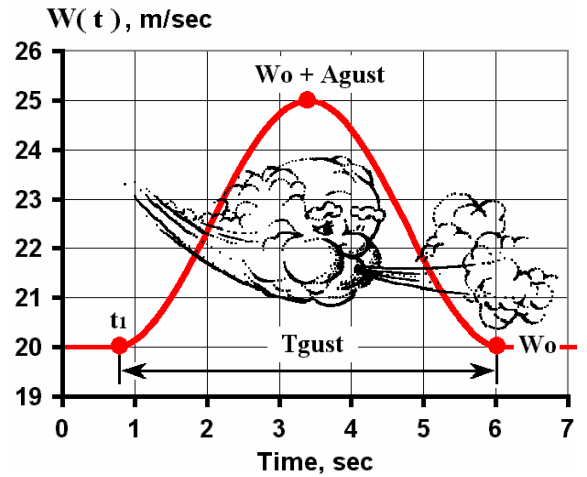


Fig.10

Ka-226. Calculations with constant rotor speed

Wind of $W_0 = 20$ m/sec with gusts to 25 m/sec versus total blade flap amplitude in comparison with the same for constant wind speeds of $W = 20$ m/sec and 25 m/sec

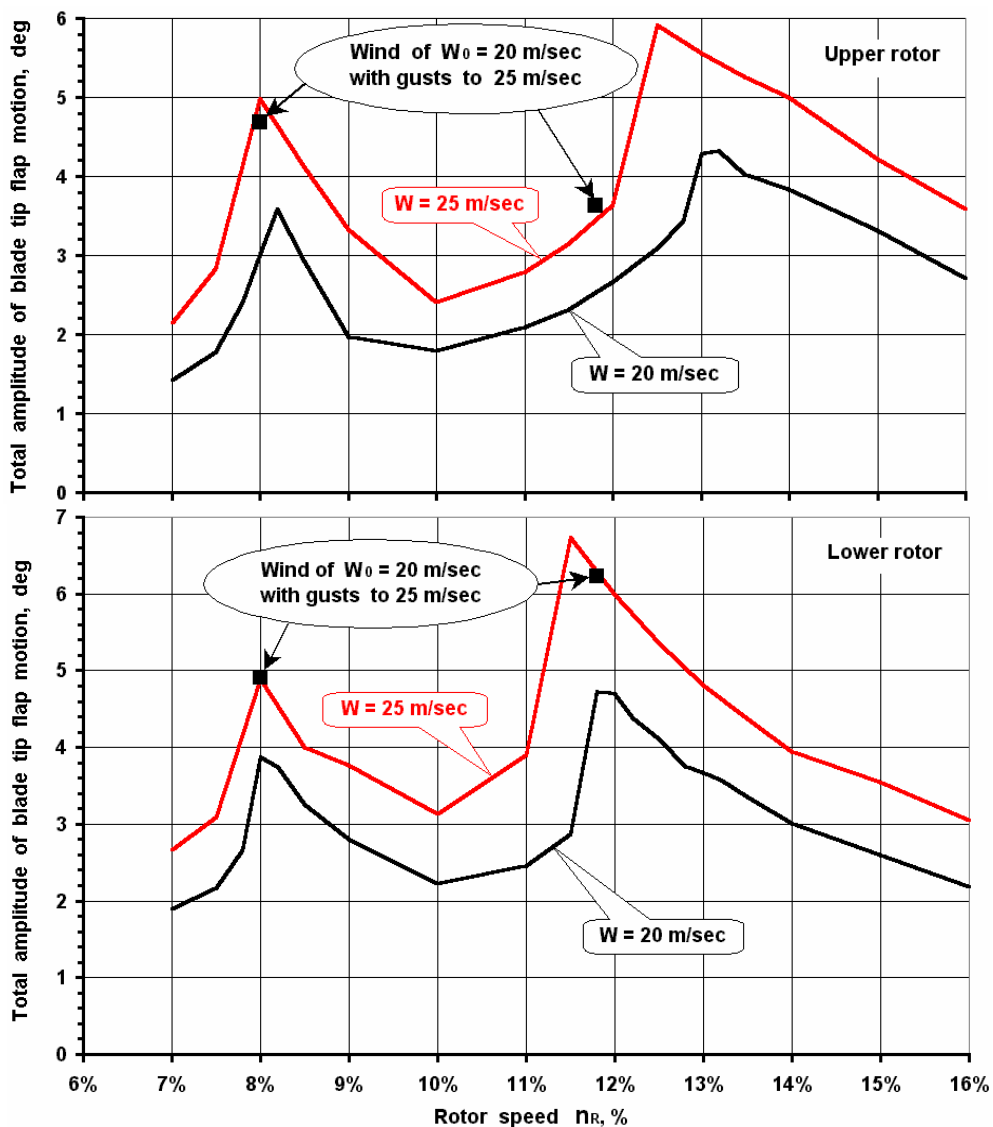


Fig.11

**Allowable wind speed diagram ($H_{min} \geq 400$ mm)
at rotor acceleration / deceleration**

Rotor speed range: $n_R = 5 \dots 40 \%$
($\varphi_{OIII} = 0^\circ$, $X_K = 0^\circ$, $X_B = 0^\circ$, $X_H = 0^\circ$)

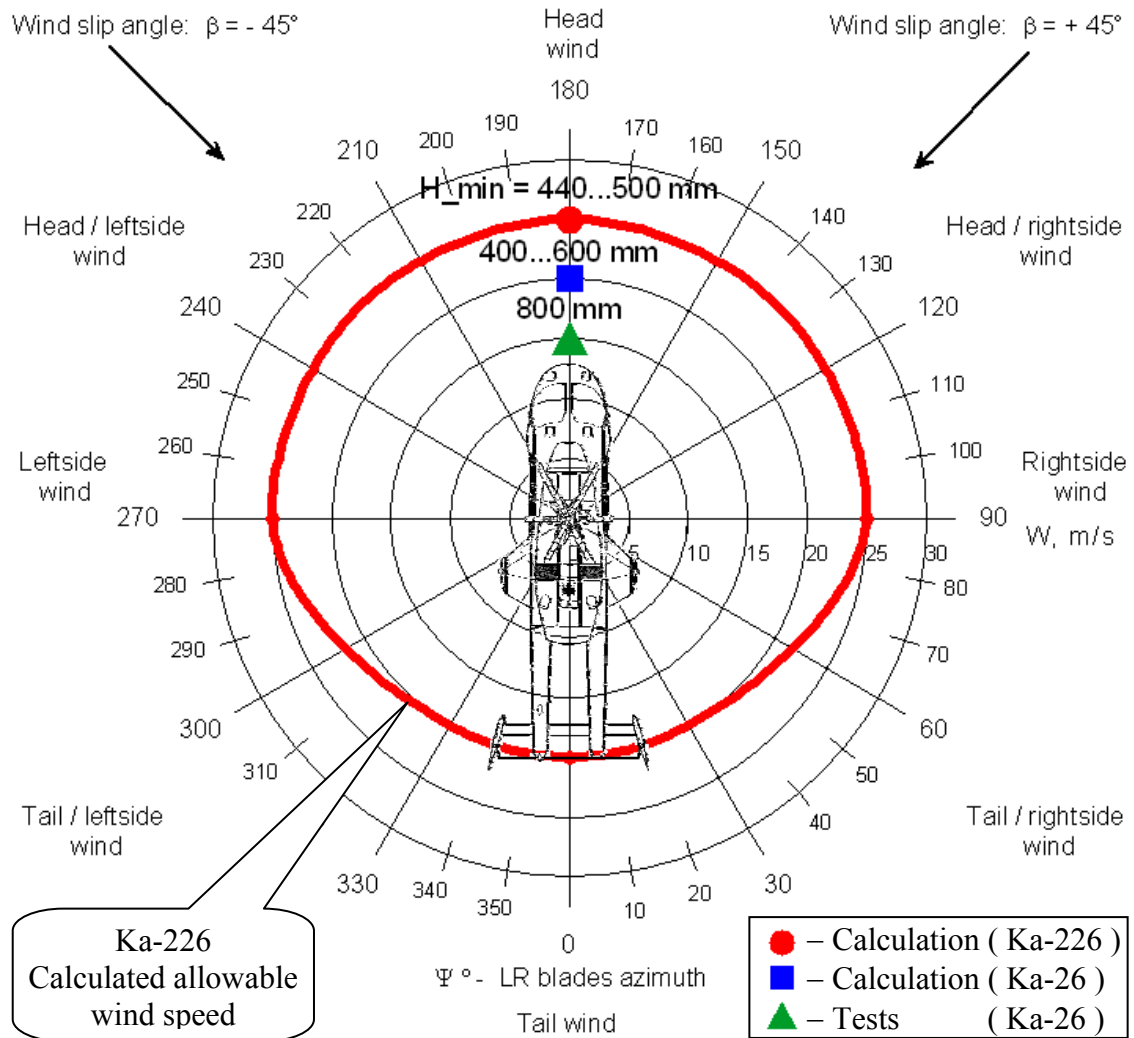


Fig.12